

Article

Future Projections of Precipitation Extremes for Greece Based on an Ensemble of High-Resolution Regional Climate Model Simulations

Prodromos Zanis ^{1,*}, Aristeidis K. Georgoulas ¹, Kondylia Velikou ¹, Dimitris Akritidis ¹, Alkiviadis Kalisoras ¹ and Dimitris Melas ²

¹ Department of Meteorology and Climatology, School of Geology, Aristotle University of Thessaloniki, 54124 Thessaloniki, Greece; ageor@auth.gr (A.K.G.); kvelikou@geo.auth.gr (K.V.); dakritid@geo.auth.gr (D.A.); kalisort@geo.auth.gr (A.K.)

² Laboratory of Atmospheric Physics, School of Physics, Aristotle University of Thessaloniki, 54124 Thessaloniki, Greece; melas@auth.gr

* Correspondence: zanis@geo.auth.gr; Tel.: +30-231-099-8240

Abstract: An assessment of the projected changes in precipitation extremes for the 21st century is presented here for Greece and its individual administrative regions. The analysis relies on an ensemble of high-resolution Regional Climate Model (RCM) simulations following various Representative Concentration Pathways (RCP2.6, RCP4.5, and RCP8.5). The simulated changes in future annual total precipitation (PRTOT) under the examined scenarios are generally negative but statistically non-robust, except towards the end of the century (2071–2100) over high-altitude mountainous regions in Western Greece, Peloponnese, and Crete under RCP8.5. The pattern of change in the number of very heavy precipitation days (R20) is linked to the respective pattern of the PRTOT change with a statistically robust decrease of up to -5 days per year only over parts of the high-altitude mountainous regions in Western Greece, Peloponnese, and Crete for 2071–2100 under RCP8.5. Contrasting the future tendency for decrease in total precipitation and R20, the changes in the intensity of precipitation extremes show a tendency for intensification. However, these change patterns are non-robust for all periods and scenarios. Statistical significance is indicated for the highest 1-day precipitation amount in a year (Rx1day) for the administrative regions of Thessaly, Central Greece, Ionian Islands, and North Aegean under RCP8.5 in 2071–2100. The changes in the contribution of the wettest day per year to the annual total precipitation (RxTratio) are mainly positive but non-robust for most of Greece and all scenarios in the period 2021–2050, becoming more positive and robust in 2071–2100 for RCP8.5. This work highlights the necessity of taking into consideration high-resolution multi-model RCM estimates in future precipitation extremes with various scenarios, for assessing their potential impact on flood episodes and the strategic planning of structure resilience at national and regional level under the anticipated human-induced future climate change.

Keywords: climate change; precipitation; indices of extremes; Regional Climate Models; Greece



Citation: Zanis, P.; Georgoulas, A.K.; Velikou, K.; Akritidis, D.; Kalisoras, A.; Melas, D. Future Projections of Precipitation Extremes for Greece Based on an Ensemble of High-Resolution Regional Climate Model Simulations. *Atmosphere* **2024**, *15*, 601. <https://doi.org/10.3390/atmos15050601>

Academic Editor: Stefano Federico

Received: 1 April 2024

Revised: 10 May 2024

Accepted: 12 May 2024

Published: 14 May 2024



Copyright: © 2024 by the authors. Licensee MDPI, Basel, Switzerland. This article is an open access article distributed under the terms and conditions of the Creative Commons Attribution (CC BY) license (<https://creativecommons.org/licenses/by/4.0/>).

1. Introduction

The Mediterranean is considered one of the most sensitive and vulnerable regions on Earth to anthropogenic climate change [1]. Average annual temperatures in the Mediterranean region are now almost 1.5 °C higher than during the 1880–1899 period, surpassing the current global warming trends (1.1 °C) [2]. The recent acceleration in temperature increase in the Mediterranean Basin is largely due to the dominant role of anthropogenic greenhouse gas radiative forcing in combination with the radiative role of decreasing aerosols and near-surface soil moisture [3]. Model simulations with Global Climate Models (GCMs) and Regional Climate Models (RCMs) project a sustained warming and drying of the Mediterranean region mostly for the latter decades of the 21st century for several

emission pathways [4–22]. Observed precipitation trends in the Mediterranean and Greece are characterized by high spatial and temporal variability which can be also affected by low frequency natural climate variability [23–27]. Yet, climate models clearly indicate a tendency towards reduced precipitation in the coming decades, especially towards the end of 21st century [16,18,22,28]. Furthermore, several studies focusing on changes in precipitation extremes report that the duration of drought periods will increase in the Mediterranean region in the future [7,29–31], while extreme precipitation events may intensify especially under the RCP8.5 scenario [17].

Greece, during the last few decades, has experienced an increasing number of various extreme events (fires, floods, heat waves, etc.), directly or indirectly related to climate change, with the public and political awareness about climate change continuously increasing. Weather extremes, such as heavy precipitation events, can induce severe floods with devastating socio-economic impacts. For example, very recently, the Daniel storm (4–8 September 2023) and the intense Medicane Ianos (15–21 September 2020) were such extreme weather events that resulted in record-breaking amounts of accumulated rainfall over parts of Greece, with an unprecedented footprint on the affected areas [32].

Governmental and non-governmental policy and decision makers, along with private and the public sector end-users, need spatially detailed information on future climate to determine the risks that anthropogenic climate change may pose. The GCMs involved in the Intergovernmental Panel on Climate Change (IPCC) fifth and sixth assessment reports still exhibit coarse spatial resolution to represent the responses of regional climate to local and regional scale forcings, like topography and land-use. Therefore, to support local/regional research on climate change impacts, alongside the development of regional strategies for adaptation and mitigation, it is essential to utilize high-resolution future climate data derived from RCMs projections. This dynamical downscaling approach is essential for the complex topography of Greece. In the framework of the “National Network on Climate Change and its Impacts (CLIMPACT)”, an assessment of projected climate change over Greece for the 21st century was carried out, using an ensemble of 11 high-resolution EURO-CORDEX RCM simulations [22]. Here, an assessment of projected climate change over Greece for the 21st century related to indices of precipitation extremes is presented as a follow up work.

2. Data and Methodology

The analysis is based on simulations carried out in the framework of the Coordinated Regional Downscaling Experiment (CORDEX) research program (<https://cordex.org/>, accessed on 1 March 2024). The simulations cover the EURO-CORDEX domain at a high horizontal resolution ($0.11^\circ \times 0.11^\circ$) spanning from 1950 to 2100 [33–35]. The historical period refers to 1950–2005, while the future projection period refers to 2006–2100 under the influence of three greenhouse gas emission scenarios; the Representative Concentration Pathways (RCPs), RCP8.5 with no further mitigation, RCP4.5 with moderate mitigation, and RCP2.6 with strong mitigation measures [36]. Each scenario describes a future pathway of greenhouse gas concentrations up to the year 2100 and the associated potential radiative forcing relative to the pre-industrial period. The simulations are a product of various Regional Climate Models (RCMs) driven by Global Climate Models (GCMs) as shown in Table 1. The selection was based on the fact that each combination of GCM-RCM provided a complete set of high-resolution simulations for the historical period and the future period under all three different RCPs. Each individual RCM simulation has its own uncertainties arising from their different parameterizations and dynamical cores as well as lateral boundary conditions from the different GCMs. The data from the 11 simulations were combined to construct an ensemble dataset for both the historical and the future (for each RCP) periods. Thus, the use of different RCM simulations results in a multi-model ensemble from which can be derived the inter-model range and uncertainty of the historical and future projections for each scenario. Daily precipitation data from each simulation were used to derive annual total precipitation (PRTOT) and extreme precipitation indices,

such as R20 (number of very heavy precipitation days in a year), Rx1day (highest 1-day precipitation amount in a year), Rx5day (highest consecutive 5-day precipitation amount in a year), and RxTratio (ratio of Rx1day to PRTOT), as described in Table 2. The indices of extreme precipitation were estimated for all 11 RCM simulations and then their average was calculated to create the ensemble mean values. The projected changes in these climate related parameters for Greece are presented for the 30-year periods of 2021–2050 (near-future) and 2071–2100 (end-of-the-century) with respect to the 1971–2000 reference period following the same set up in the selected periods as in the work by Georgoulas et al. [22], Mavromatis et al. [28], and Rovithakis et al. [37] in the framework of CLIMPACT for consistency reasons.

Table 1. List of the RCM simulations including the name of the RCM, the driving GCM and the realization. All simulations were carried out for the historical period 1950–2005 and the future period 2006–2100 under the influence of RCP2.6, RCP4.5, and RCP8.5. Source of RCM simulations: <https://esgf-node.llnl.gov/search/esgf-llnl/> (accessed on 1 March 2024).

	RCM	Driving GCM	Realization
1	ALADIN63.v2	CNRM.CNRM-CERFACS-CNRM-CM5	r1i1p1
2	CCLM4-8-17.v1	CLMcom.ICHEC-EC-EARTH	r12i1p1
3	HIRHAM5.v2	DML.ICHEC-EC-EARTH	r3i1p1
4	RACMO22E.v1	KNMI.ICHEC-EC-EARTH	r12i1p1
5	RACMO22E.v2	KNMI.MOHC-HadGEM2-ES	r1i1p1
6	RACMO22E.v2	KNMI.CNRM-CERFACS-CNRM-CM5	r1i1p1
7	RCA4.v1	SMHI.MOHC-HadGEM2-ES	r1i1p1
8	RCA4.v1	SMHI.MPI-M-MPI-ESM-LR	r1i1p1
9	RCA4.v1	SMHI.ICHEC-EC-EARTH	r12i1p1
10	REMO2009.v1	MPI-CSC.MPI-M-MPI-ESM-LR	r1i1p1
11	REMO2009.v1	MPI-CSC.MPI-M-MPI-ESM-LR	r2i1p1

Table 2. Extreme precipitation indices calculated within CLIMPACT for an ensemble of 11 EURO-CORDEX RCMs for the period 1950–2100.

	Precipitation Index	Definition
1	R20 (Very Heavy Precipitation Days)	Number of days in a year with daily precipitation > 20 mm
2	Rx1day (Highest 1-day Precipitation Amount)	The day with the highest precipitation in a year
3	Rx5day (Highest 5-day Precipitation Amount)	Annual maximum consecutive 5-day precipitation
4	RxTratio (Ratio Rx1day/PRTOT)	The ratio between the highest precipitation in a year and annual total precipitation

The daily mean, minimum, and maximum near-surface temperature and PRTOT from the historical EURO-CORDEX simulations (used in this work) were evaluated for the reference period 1971–2000 with respect to gridded observational data at a 0.1° horizontal resolution of the European Climate Assessment & Dataset (ECA&D) gridded dataset (E-OBS) by Georgoulas et al. [22]. The E-OBS gridded dataset is based on observational data from stations all over Europe [38,39]. The mean bias (MB: difference between the mean values of two timeseries) and the normalized mean bias (NMB: percentage of the difference between the mean values of two timeseries) metrics were calculated on a grid cell basis while the statistical significance of the differences at the 95% confidence level is indicated using an independent-samples *t*-test. Furthermore, the spatial correlation between E-OBS and the EURO-CORDEX ensemble was also calculated using the spatial

Pearson's correlation coefficient (R_{spatial}). Georgoulas et al. [22] reported that the EURO-CORDEX ensemble temperature data exhibit a reasonable agreement with the gridded observational data ($MB = -0.8$ °C, $NMB = -6.9\%$, $R_{\text{spatial}} = 0.9$) while the PRTOT data show a moderate agreement as discussed below. The MB pattern of the EURO-CORDEX ensemble PRTOT relative to E-OBS is illustrated in Figure S1 along with the calculated mean values over the whole area of MB, NMB, and R_{spatial} ($MB = 241$ mm/year, $NMB = 40\%$, $R_{\text{spatial}} = 0.6$). The precipitation patterns of the ensemble and E-OBS are similar, but EURO-CORDEX ensemble overestimates PRTOT with a tendency for stronger overestimation over the high elevation mountainous areas. Our results are in line with previous studies. Kotlarski et al. [40] showed that the temperature MBs over Europe of hindcast EURO-CORDEX simulations relative to E-OBS are mostly smaller than 1.5 °C (-0.8 °C over Mediterranean), while precipitation NMBs are typically within the $\pm 40\%$ range (30% over Mediterranean). Furthermore, Katragkou et al. [41] showed similar results evaluating hindcast EURO-CORDEX simulations against E-OBS.

The statistical robustness of the differences was checked considering the ensemble's inter-model variability as discussed in Georgoulas et al. [22]. In more detail, a difference is regarded robust when at least 7 out of the 11 simulations constituting each ensemble exhibit differences with the same sign with that of the ensemble difference and are also statistically significant (at the 95% confidence level) following the non-parametric Mann–Whitney test [42]. Furthermore, the analysis of the extreme precipitation indices has also been carried out at the regional level of the administrative regions of the state of Greece, which are shown in Figure 1. This is very important as adaptation measures are commonly implemented at a regional level in the country, taking into account the special characteristics of each region. For each administrative region, the average difference between the future periods and the reference period is reported. In this case, the statistical significance is checked at the 95% confidence level applying a two-tailed two-sample t -test considering the inter-model variability. Each sample (future/reference) consists of 11 values depicting the mean value for each set of RCM simulations. Mean values and standard deviation of PRTOT, R20, Rx1day, Rx5day, and RxTratio are shown for all the 13 administrative regions in the Supplementary Materials (Tables S1–S5, respectively) for the reference period 1971–2000 and for the two future periods (2021–2050 and 2071–2100) under the three RCPs.

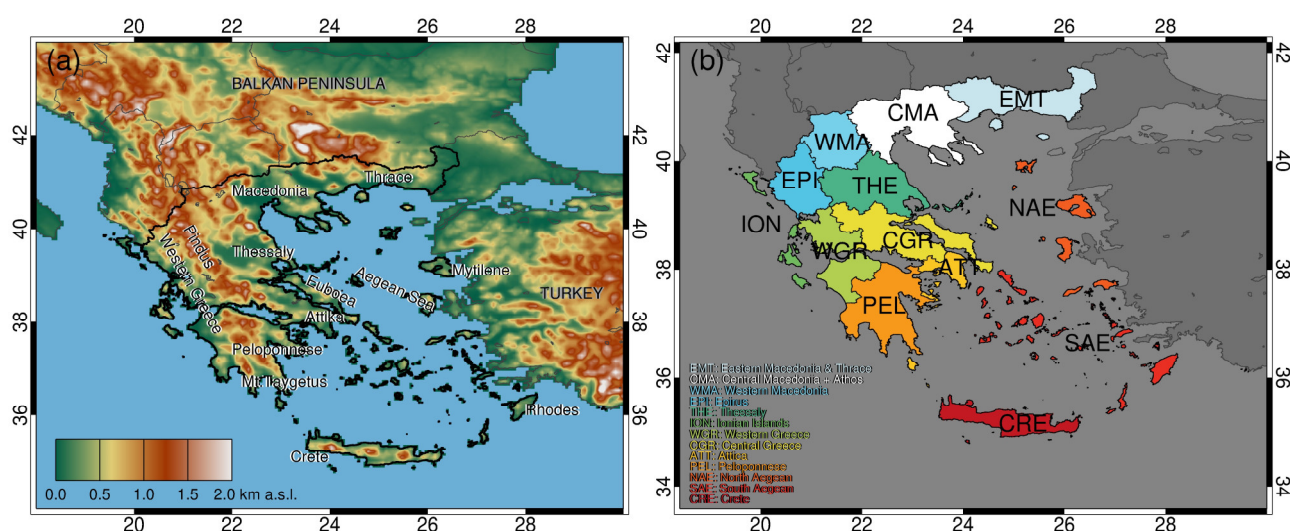


Figure 1. (a) Topography of the examined region (in kilometers above sea level—km a.s.l.). Locations and areas of interest are also indicated along with the outline of Greece. (b) Map with the borders of the thirteen administrative regions of Greece (EMT: Eastern Macedonia and Thrace; CMA: Central Macedonia + Athos; WMA: Western Macedonia; EPI: Epirus; THE: Thessaly; ION: Ionian Islands; WGR: Western Greece; CGR: Central Greece; ATT: Attica; PEL: Peloponnese; NAE: North Aegean; SAE: South Aegean; CRE: Crete).

3. Results

Figure 2 depicts the projected ensemble PRTOT change for the near-future and the end-of-the-century periods for all three RCPs on an annual basis with respect to the reference period (1971–2000). The projected changes under the three scenarios are generally statistically non-robust except at the end of the century (2071–2100) over high elevation mountainous areas in Western Greece, Peloponnese, and Crete under RCP8.5, where a large (up to about $-300 \text{ mm year}^{-1}$) statistically robust PRTOT decrease is projected.

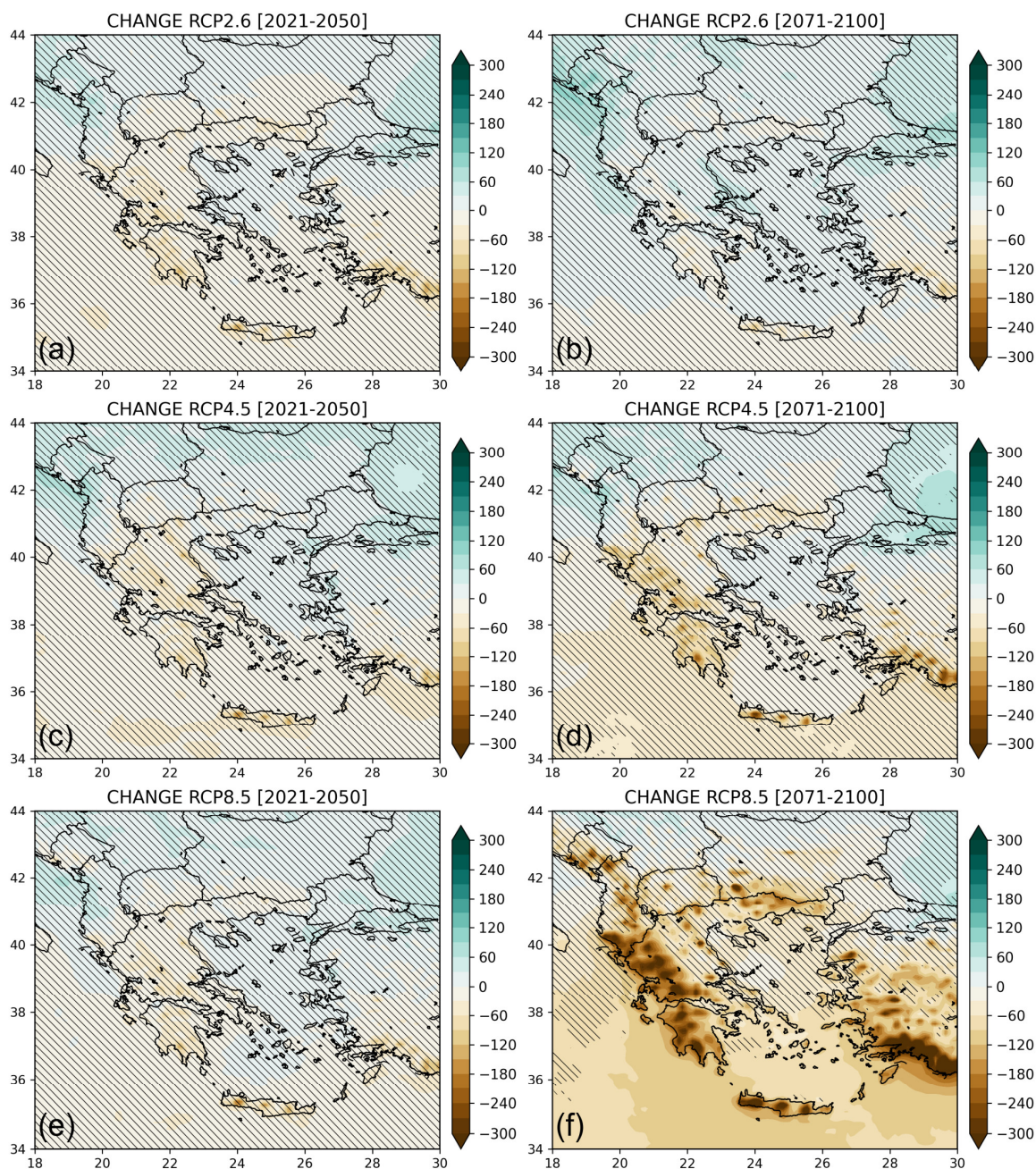


Figure 2. Difference for the PRTOT annual precipitation (mm year^{-1}) in the EURO-CORDEX ensemble for 2021–2050 and 2071–2100 with respect to the reference period (1971–2000), for RCP2.6 (a,b), RCP4.5 (c,d), and RCP8.5 (e,f). Hatched areas indicate not statistically robust differences.

The percentage changes of PRTOT for the individual administrative regions of Greece are shown in Figure 3. Specifically, for RCP2.6, a statistically non-significant at the 95% confidence level change ranging between -4.8% and $+3.2\%$ among the different admin-

istrative regions of Greece for both future periods is projected with a mean estimate for the whole Greece of -3% for 2021–2050 and $+0.5\%$ for 2071–2100. Similarly, for RCP4.5, a non-significant change ranging between -7.9% and $+0.9\%$ among the different administrative regions of Greece is projected for 2021–2050, with a mean estimate for the whole country of -3% . For 2071–2100, a non-significant decrease in PRTOT is projected for all the administrative regions of Greece ranging between -11.7% and -3.1% with a mean estimate for the whole Greece of -5.9% . Similar change patterns are found for RCP8.5 with respect to the other two scenarios for the 2021–2050 period with small non-significant changes ranging between -7.8% and $+0.5\%$ among the different regions in Greece and a mean estimate for the whole country of -2.7% . However, for the end of the century (2071–2100) a statistically robust decrease of PRTOT is projected over extended parts of Greece for RCP8.5 (Figure 2) with values ranging between -26.5% and -10.7% among the different administrative regions and a mean estimate for the whole Greece of -16% . Notable is the statistically significant decrease of PRTOT for the administrative regions of Western Greece, Attica, South Aegean, and Crete (Figure 3).

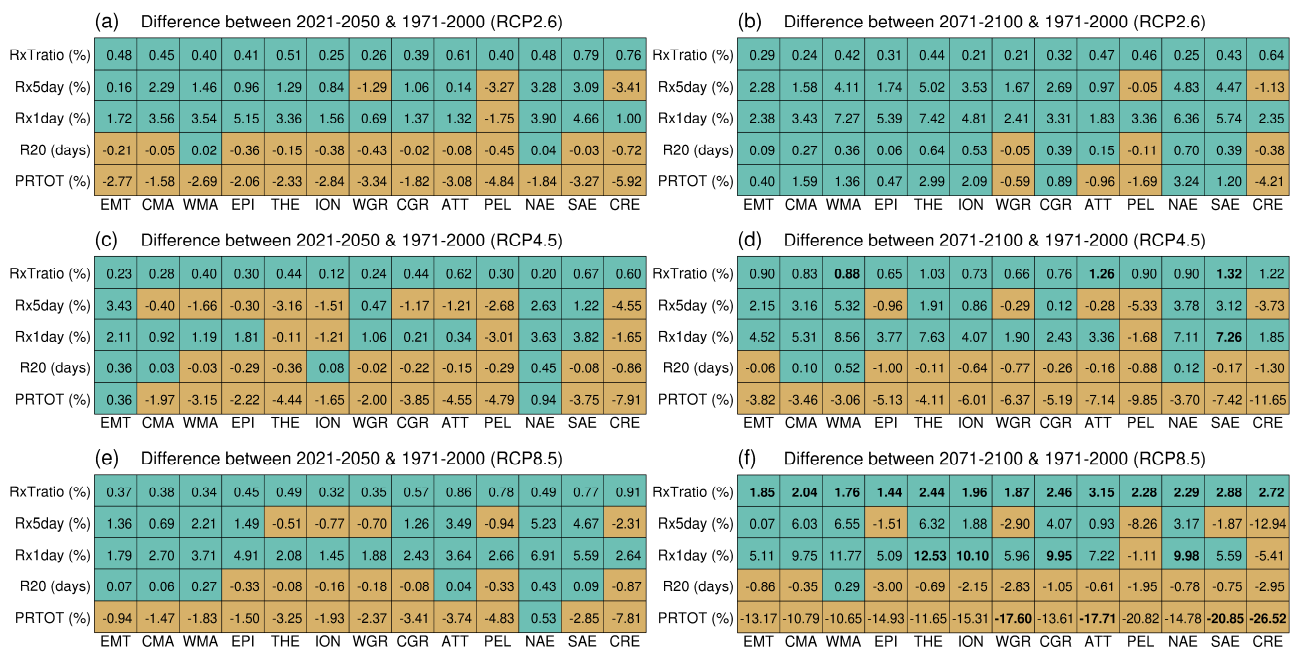


Figure 3. Heatmaps with the differences between the periods 2021–2050 and 1971–2000 (a) and 2071–2100 and 1971–2000 (b) under RCP2.6 (a,b), RCP4.5 (c,d), and RCP8.5 (e,f) of PRTOT and all the examined extreme precipitation indices (R20, Rx1day, Rx5day, and RxTratio) for each one of the thirteen administrative regions of Greece (EMT: Eastern Macedonia and Thrace; CMA: Central Macedonia and Athos; WMA: Western Macedonia; EPI: Epirus; THE: Thessaly; ION: Ionian Islands; WGR: Western Greece; CGR: Central Greece; ATT: Attica; PEL: Peloponnese; NAE: North Aegean; SAE: South Aegean; CRE: Crete). Cyan color indicates positive, and brown negative, differences. The values in bold indicate statistically significant results at the 95% confidence level based on a two-tailed two-sample *t*-test taking into account the inter-model variability.

Figure 4 depicts the spatial changes in R20 (number of very heavy precipitation days per year with daily precipitation > 20 mm) for the periods 2021–2050 and 2071–2100 with respect to the reference period. In general, the patterns of R20 change are linked to the respective patterns of the PRTOT change. In most scenarios, there are non-robust small changes in R20 ranging between -2 and $+2$ days per year. A statistically robust decrease up to -5 days per year appears for the frequency of very heavy precipitation days only over parts of high-altitude mountainous regions of Western Greece, Peloponnese, and Crete for the 2071–2100 period under RCP8.5, which are areas also exhibiting a robust decrease in PRTOT (Figure 4). It is noticed in Figure 3 that the changes in R20 are very small

and non-significant for all the administrative regions of Greece for the near future period (2021–2050) under all the examined scenarios. The strongest but non-significant change is revealed in Crete (decrease of -0.7 to -0.9 days per year for the three RCP scenarios). For the period 2071–2100, the changes in R20 are similarly very small and non-robust across all the administrative regions of Greece for all the examined scenarios. For RCP4.5, the largest change is revealed in the administrative regions of Epirus and Crete with a decrease of -1.0 and -1.3 days per year, respectively. The decrease in R20 becomes stronger for RCP8.5 over 2071–2100, with a decrease of roughly more than 2 days per year, in the administrative regions of Epirus, Western Greece, Peloponnese, and Crete.

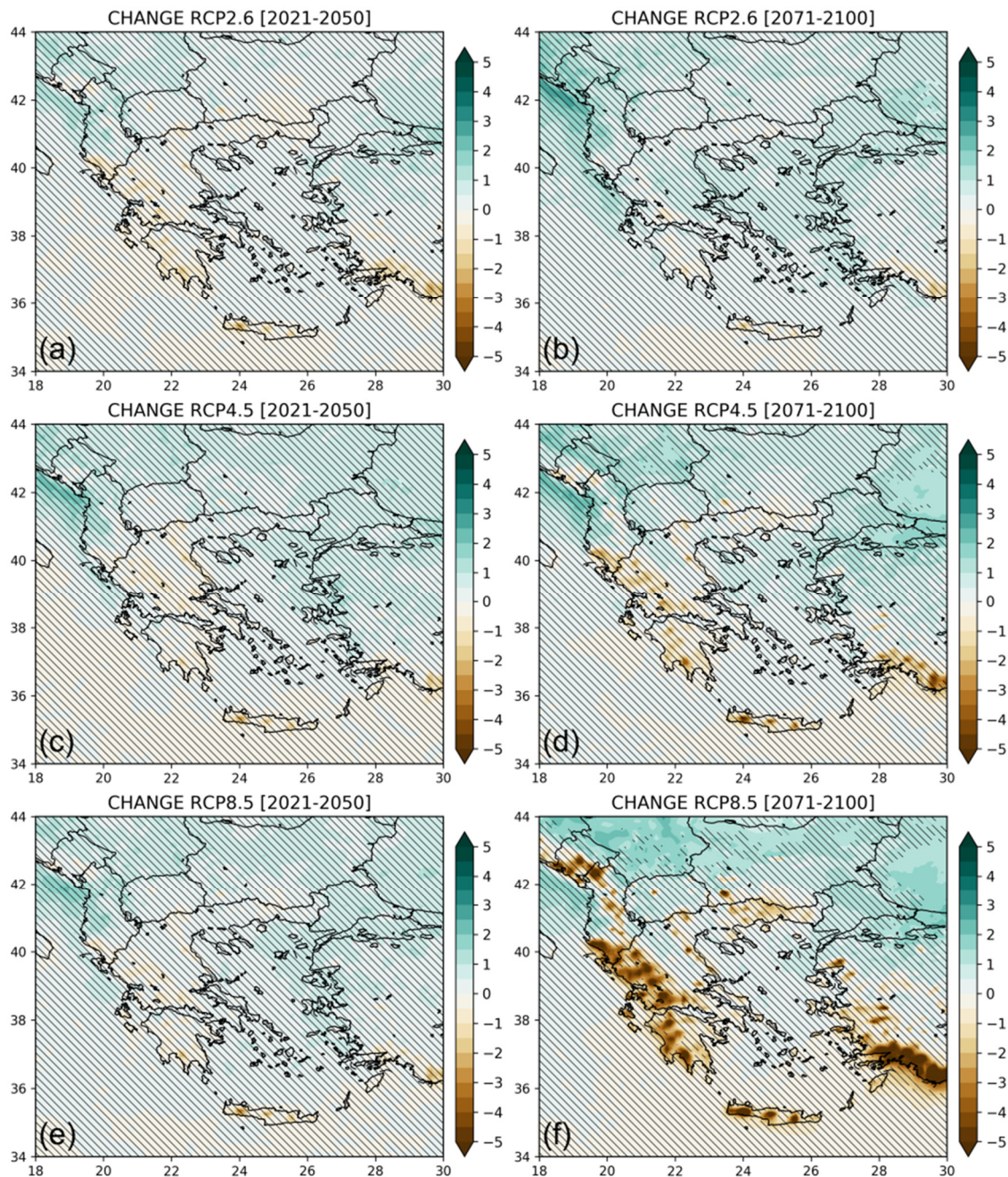


Figure 4. Similar to Figure 2 but for the index R20 (number of very heavy precipitation days per year) in the EURO-CORDEX ensemble for 2021–2050 and 2071–2100 with respect to the reference period (1971–2000), for RCP2.6 (a,b), RCP4.5 (c,d), and RCP8.5 (e,f).

Despite the tendency for a decrease in total precipitation and in the frequency of very heavy precipitation events, as indicated from Figures 2 and 4, especially over the end of the century period 2071–2100, the extreme precipitation indices Rx1day and Rx5day show a tendency for intensification in the future, yet, with the changes being non-robust for all periods and scenarios (Figures 5 and 6).

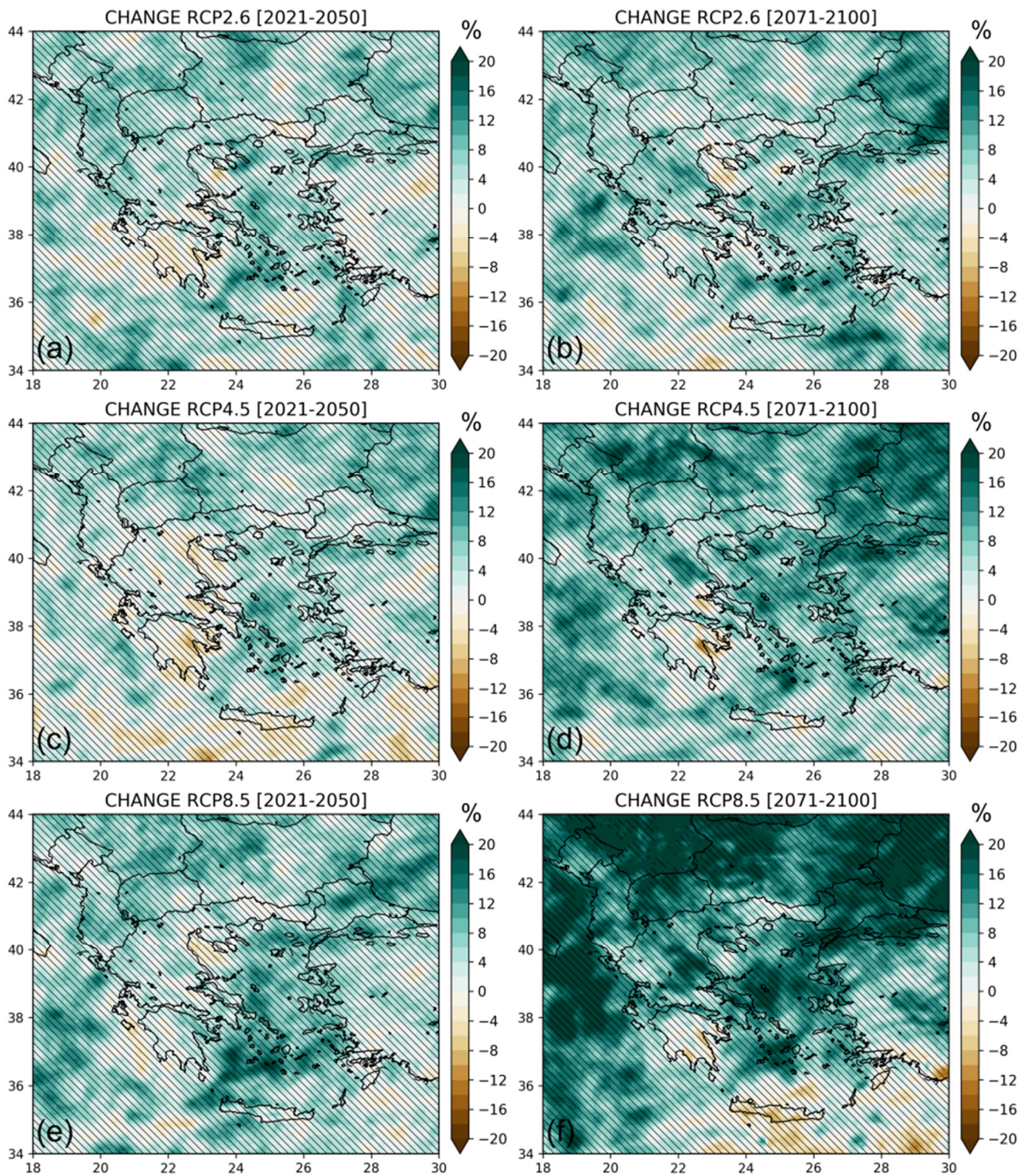


Figure 5. Percentage difference [$100 \times (\text{future period} - \text{reference period}) / \text{reference period}$] for the index Rx1day (Highest 1-day Precipitation amount per year) in the EURO-CORDEX ensemble for 2021–2050 and 2071–2100 with respect to the reference period (1971–2000), for RCP2.6 (a,b), RCP4.5 (c,d), and RCP8.5 (e,f). Hatched areas indicate not statistically robust differences.

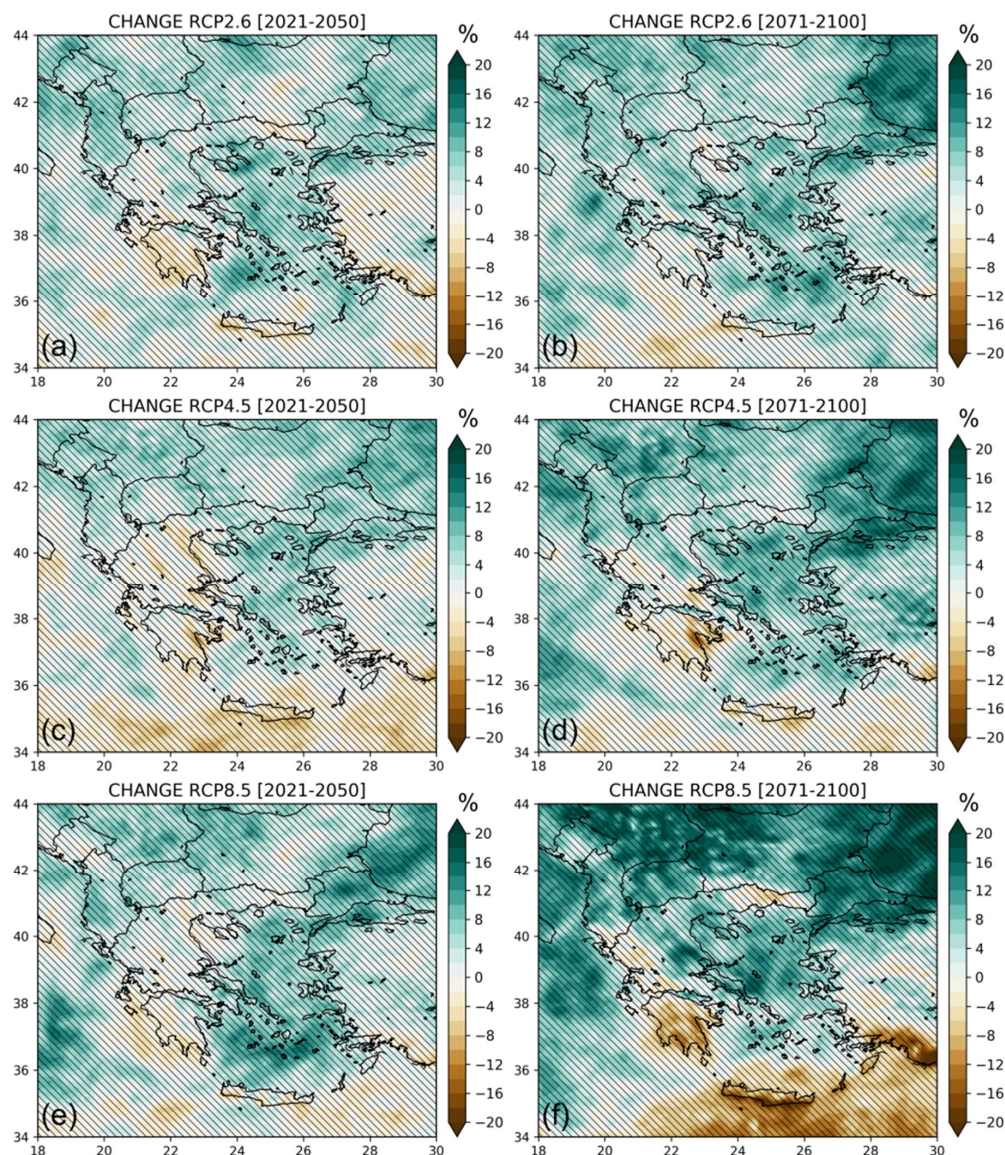


Figure 6. Similar to Figure 5 but for the index Rx5day (highest consecutive 5-day precipitation amount per year) in the EURO-CORDEX ensemble for 2021–2050 and 2071–2100 with respect to the reference period (1971–2000), for RCP2.6 (a,b), RCP4.5 (c,d), and RCP8.5 (e,f).

It is noticed in Figure 3 that the changes in Rx1day and Rx5day are very small (statistically non-significant) but mostly positive for all the administrative regions of Greece for the near future period for all the scenarios, with the strongest positive change projected in North and South Aegean. Specifically for these two administrative regions, a consistent increase from 3.6 to 6.9% in Rx1day and from 1.2 to 5.2% in Rx5day is projected for the three RCPs. The region of Crete is an exception with the Rx5day index decreasing from -2.3 to -4.6% under the three RCPs.

For the period 2071–2100, the changes in Rx1day and Rx5day are mainly positive but statistically non-significant over the majority of the country's administrative regions under all the examined RCPs, with exceptions towards the southern latitudes (Peloponnese and Crete) where negative changes are projected. It is worth pointing out that the strongest increases in Rx1day are projected for the administrative regions of Thessaly (from 7.4 to 12.5%), Western Macedonia (from 7.3 to 11.8%), and North Aegean (from 6.4 to 10%) for all the examined RCPs. Statistically significant increases in Rx1day are found mainly for RCP8.5 in 2071–2100 for the administrative regions of Thessaly (12.5%), Central Greece (10%), Ionian Islands (10%), and North Aegean (10%). It is also worth mentioning that

the strongest (but statistically non-significant) decreases in Rx5day are projected for Crete (-12.9%) and Peloponnese (-8.3%) for RCP8.5 in the 2071–2100 period. As an example, to illustrate visually the inter-model variability of historical and future simulations under the different scenarios, Figure S2 shows the timeseries (1950–2100) of the percentage difference of Rx1day with respect to the reference period (1971–2000) for the 13 subregions of Greece.

Figure 7 shows the changes in the RxTratio (ratio of Rx1day to PRTOT) index which is sensitive to changes in both Rx1day and PRTOT and hence should be interpreted considering the combination of the changes discussed in Figure 2 for PRTOT and Figure 5 for Rx1day.

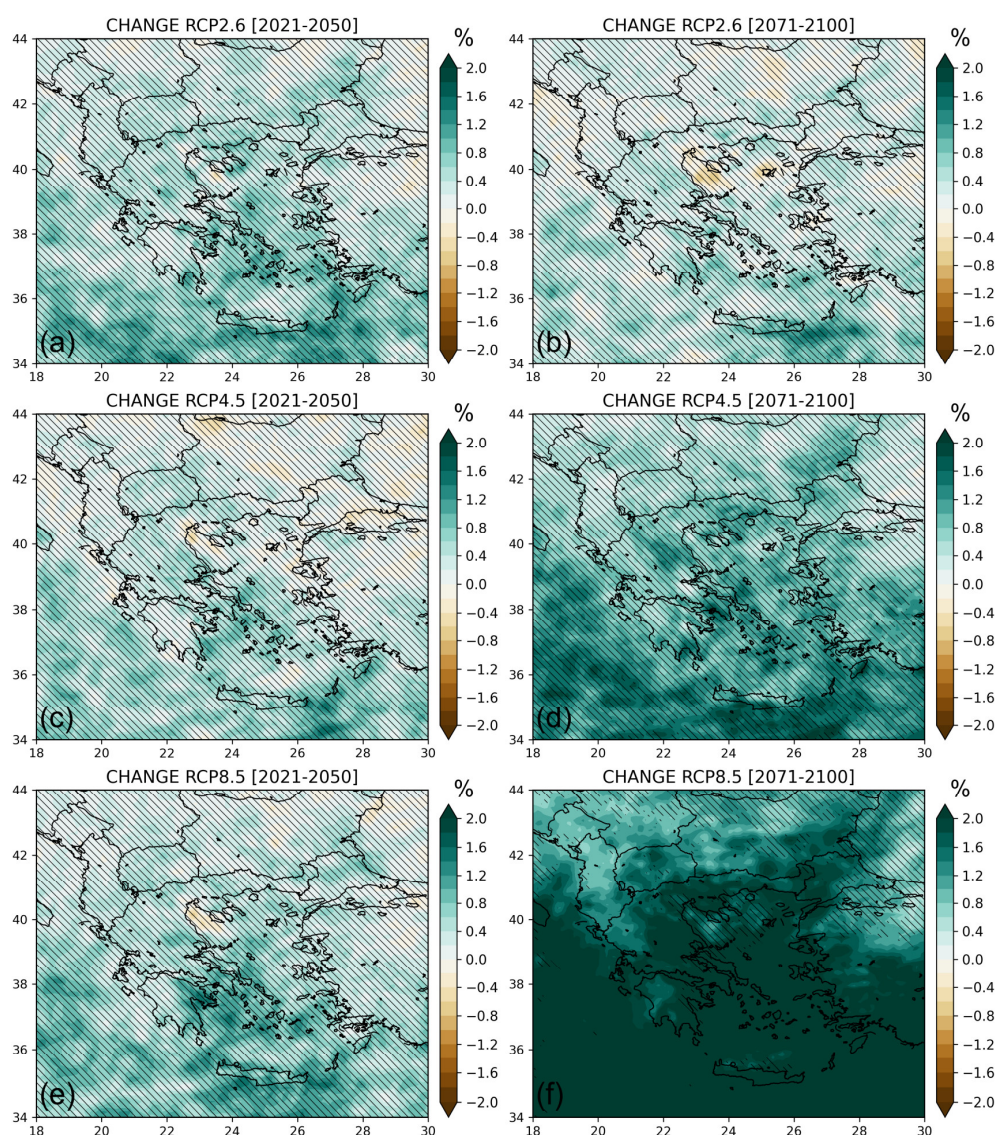


Figure 7. Similar to Figure 2 but for the index $100 \times \text{RxTratio}$ (%) (Ratio of Rx1day to PRTOT) in the EURO-CORDEX ensemble for 2021–2050 and 2071–2100 with respect to the reference period (1971–2000), for RCP2.6 (a,b), RCP4.5 (c,d), and RCP8.5 (e,f).

The changes in RxTratio are mainly positive but non-robust for most of Greece and all the scenarios in the period 2021–2050 and become more positive near the end of the century especially for RCP8.5 with robust positive changes almost all over the whole country. This behavior with the tendency of RxTratio values getting more positive upon the latter part of the century can be interpreted by the tendency of Rx1day and PRTOT values to increase and decrease, respectively. Presumably, the ratio is more sensitive to the changes of the denominator PRTOT, and this is the reason that the robust positive changes of RxTratio for RCP8.5 are determined by the robust negative changes of PRTOT for RCP8.5.

4. Conclusions and Discussion

The aim of this work is a multi-model assessment of high-resolution projections for three Representative Concentration Pathways (RCP2.6, RCP4.5, and RCP8.5) over the 21st century in precipitation extremes (in terms of frequency and intensity) for Greece as well as, for the first time to our knowledge, for its individual administrative regions.

The projected changes of the annual total precipitation (PRTOT) under the three RCP scenarios are generally negative but statistically non-robust except at the end of the century (2071–2100) over high-altitude mountainous regions in Western Greece, Peloponnese, and Crete under RCP8.5. The decrease of PRTOT in the future over Greece, reported here, is in accordance with previous RCM ensemble studies focusing over the Mediterranean Basin [16,17,20,33] or Greece [9,12,22,28]. Coppola et al. [20], based on a 55-member ensemble of high-resolution (0.11°) RCM simulations showed negative changes of precipitation in the Mediterranean of about -10% for 2041–2070 and -22% for 2071–2100 under RCP8.5. Zittis et al. [17] using an ensemble of 33 high-resolution (0.11°) RCM simulations for RCP8.5 indicated PRTOT changes in the range of 0 to -10% for 2001–2050 and in the range of 0 to -30% for 2051–2100 with the largest decreases towards the southern parts of Greece (Peloponnese and Crete). Also, Zittis et al. [16], using ensembles of RCM simulations (at 0.44° spatial resolution) for three scenarios (RCP2.6, RCP4.5, and RCP8.5) from several CORDEX domains including the Mediterranean, showed similar estimates for the PRTOT decrease over Greece in comparison to our estimates for the different scenarios and future periods.

The patterns of change in the number of very heavy precipitation days per year (R20) are linked to the respective patterns of the PRTOT change with a statistically robust decrease of up to -5 days per year over parts of the high-altitude mountainous regions in Western Greece, Peloponnese, and Crete for the end-of-the-century period under RCP8.5. Generally, the changes in R20 are very small and non-significant over all the administrative regions for both future periods and under all the examined scenarios. Among the administrative regions of Greece, the largest decrease (roughly more than -2 days per year), is projected at Epirus, Western Greece, Peloponnese, and Crete, for RCP8.5 over the end century period.

Despite the tendency for decrease in total precipitation and in the frequency of very heavy precipitation days, the indices of extreme precipitation Rx1day and Rx5day show a tendency for intensification in the future, but the changes are mostly non-robust for all periods and scenarios. Robust increases in Rx1day are calculated mainly for RCP8.5 in 2071–2100 for the administrative regions of Thessaly (12.5%), Central Greece (10%), Ionian Islands (10%), and North Aegean (10%). However, there are exceptions towards the southern latitudes with worth-mentioning negative changes in Rx5day projected for Crete (-12.9%) and Peloponnese (-8.3%) for RCP8.5 in the 2071–2100 period.

The changes in the ratio Rx1day/PRTOT (RxTratio) are mainly positive but non-robust for most of Greece and all scenarios in the period 2021–2050 and become more positive towards the end of the century (2071–2100), especially for RCP8.5 that indicates robust positive changes for all the administrative regions of Greece. The contribution of the wettest day per year to the annual total precipitation is projected to increase by roughly up to 2% throughout Greece towards the end of the century (2071–2100) under RCP8.5. This behavior can be interpreted by the fact that Rx1day values tend to increase while PRTOT values tend to decrease.

Our analysis is in line with the multi-model studies of Coppola et al. [20] and Zittis et al. [17]. Coppola et al. [20] showed a pattern with positive changes in Rx1day and Rx5day over central and north Greece and negative values towards southern Greece (Peloponnese and Crete) for 2071–2100 under RCP8.5. Zittis et al. [17] showed also that extreme precipitation events may intensify in the future under an RCP8.5 scenario with the 50-year maximum daily precipitation (Rx1day) increasing by 0–50% over Greece for 2051–2100, while the contribution of the most wet day per year to the annual total precipitation is projected to increase from 2% to 6%.

Overall, this analysis points towards a possibly drier future climate characterized by a non-robust tendency with less frequent but more intense extreme precipitation events, while statistically significant and robust results are projected only for the end-of-the-century period under RCP8.5. This work highlights the need of including multi-model ensemble estimates of future climate projections from various RCMs and under different scenarios on studying precipitation extremes and the potential impact they may have on flood episodes in accordance with the structure resilience at national and regional level under the anticipated anthropogenic future climate change. The above-mentioned multi-approach could be implemented in the calculation of Intensity-Duration-Frequency (IDF) precipitation curves for the update of flood risk management plans at catchment areas of the administrative regions of Greece.

Supplementary Materials: The following supporting information can be downloaded at: <https://www.mdpi.com/article/10.3390/atmos15050601/s1>, Table S1: PR1OT (pages 3–5); Table S2: R20 (pages 6–8); Table S3: Rx1day (pages 9–11); Table S4: Rx5day (pages 12–14); Table S5: RxTratio (pages 15–17); Figure S1: MB (page 18); Figure S2: Rx1day (pages 19–23).

Author Contributions: Conceptualization, P.Z. and A.K.G.; methodology, A.K.G., K.V., D.A. and P.Z.; software, D.A., A.K.G., A.K. and K.V.; validation, A.K.G. and A.K.; formal analysis, D.A., A.K.G. and K.V.; investigation, A.K.G., K.V., D.A. and P.Z.; data curation, D.A., A.K.G., A.K. and K.V.; writing—original draft preparation, P.Z. and A.K.G.; writing—review and editing, A.K.G., K.V., D.A., A.K., D.M. and P.Z.; visualization, A.K.G., D.A. and K.V.; project administration, D.M. and P.Z. All authors have read and agreed to the published version of the manuscript.

Funding: This research was funded by the project “Support for Enhancing the Operation of the National Network for Climate Change (CLIMPACT)”, National Development Program, General Secretariat of Research and Innovation, Greece (2023NA11900001—N. 5201588).

Institutional Review Board Statement: Not applicable.

Informed Consent Statement: Not applicable.

Data Availability Statement: The EURO-CORDEX simulations used for the analysis are publicly available via <https://esgf-data.dkrz.de/search/cordex-dkrz/> (accessed on 1 March 2024).

Acknowledgments: We acknowledge the World Climate Research Program’s Working Group on Regional Climate, and the Working Group on Coupled Modelling, former coordinating body of CORDEX and responsible panel for CMIP5. We also thank the climate modeling groups (listed in Table 1) for producing and making available their model output. We also acknowledge the Earth System Grid Federation infrastructure an international effort led by the U.S. Department of Energy’s Program for Climate Model Diagnosis and Intercomparison, the European Network for Earth System Modelling and other partners in the Global Organization for Earth System Science Portals (GO-ESSP).

Conflicts of Interest: The authors declare no conflicts of interest.

References

1. Giorgi, F. Climate Change Hot-Spots. *Geophys. Res. Lett.* **2006**, *33*, L08707. [CrossRef]
2. Cramer, W.; Guiot, J.; Fader, M.; Garrabou, J.; Gattuso, J.-P.; Iglesias, A.; Lange, M.A.; Lionello, P.; Llasat, M.C.; Paz, S.; et al. Climate Change and Interconnected Risks to Sustainable Development in the Mediterranean. *Nat. Clim. Chang.* **2018**, *8*, 972–980. [CrossRef]
3. Urdiales-Flores, D.; Zittis, G.; Hadjinicolaou, P.; Osipov, S.; Klingmüller, K.; Mihalopoulos, N.; Kanakidou, M.; Economou, T.; Lelieveld, J. Drivers of Accelerated Warming in Mediterranean Climate-Type Regions. *npj Clim. Atmos. Sci.* **2023**, *6*, 97. [CrossRef]
4. Gibelin, A.-L.; Déqué, M. Anthropogenic Climate Change over the Mediterranean Region Simulated by a Global Variable Resolution Model. *Clim. Dyn.* **2003**, *20*, 327–339. [CrossRef]
5. Gao, X.; Pal, J.S.; Giorgi, F. Projected Changes in Mean and Extreme Precipitation over the Mediterranean Region from a High Resolution Double Nested RCM Simulation. *Geophys. Res. Lett.* **2006**, *33*, L03706. [CrossRef]
6. Diffenbaugh, N.S.; Pal, J.S.; Giorgi, F.; Gao, X. Heat Stress Intensification in the Mediterranean Climate Change Hotspot. *Geophys. Res. Lett.* **2007**, *34*, L11706. [CrossRef]
7. Goubanova, K.; Li, L. Extremes in Temperature and Precipitation around the Mediterranean Basin in an Ensemble of Future Climate Scenario Simulations. *Glob. Planet. Change* **2007**, *57*, 27–42. [CrossRef]
8. Giorgi, F.; Lionello, P. Climate Change Projections for the Mediterranean Region. *Glob. Planet. Change* **2008**, *63*, 90–104. [CrossRef]

9. Zanis, P.; Kapsomenakis, I.; Philandras, C.; Douvis, K.; Nikolakis, D.; Kanellopoulou, E.; Zerefos, C.; Repapis, C. Analysis of an Ensemble of Present Day and Future Regional Climate Simulations for Greece. *Int. J. Climatol.* **2009**, *29*, 1614–1633. [\[CrossRef\]](#)
10. Öñol, B.; Semazzi, F.H.M. Regionalization of Climate Change Simulations over the Eastern Mediterranean. *J. Clim.* **2009**, *22*, 1944–1961. [\[CrossRef\]](#)
11. Zerefos, C.; Repapis, C.; Giannakopoulos, C.; Kapsomenakis, J.; Papanikolaou, D.; Papanikolaou, M.; Poulos, S.; Vrekoussis, M.; Philandras, C.; Tselioudis, G.; et al. The Climate of the Eastern Mediterranean and Greece: Past, Present and Future. In *The Environmental, Economic and Social Impacts of Climate Change in Greece*; Climate Change Impacts Study Committee, Bank of Greece: Athens, Greece, 2011; pp. 1–126. ISBN 978-960-7032-49-2.
12. Tolika, K.; Zanis, P.; Anagnostopoulou, C. Regional Climate Change Scenarios for Greece: Future Temperature and Precipitation Projections from Ensembles of RCMs. *Glob. Nest J.* **2012**, *14*, 407–421.
13. Lelieveld, J.; Hadjinicolaou, P.; Kostopoulou, E.; Giannakopoulos, C.; Pozzer, A.; Tanarhte, M.; Tyrlis, E. Model Projected Heat Extremes and Air Pollution in the Eastern Mediterranean and Middle East in the Twenty-First Century. *Reg. Environ. Chang.* **2014**, *14*, 1937–1949. [\[CrossRef\]](#)
14. Öñol, B.; Bozkurt, D.; Turuncoglu, U.U.; Sen, O.L.; Dalfes, H.N. Evaluation of the Twenty-First Century RCM Simulations Driven by Multiple GCMs over the Eastern Mediterranean–Black Sea Region. *Clim. Dyn.* **2014**, *42*, 1949–1965. [\[CrossRef\]](#)
15. Zanis, P.; Katragkou, E.; Ntogras, C.; Marougianni, G.; Tsikerdekis, A.; Feidas, H.; Anadranistakis, E.; Melas, D. Transient High-Resolution Regional Climate Simulation for Greece over the Period 1960–2100: Evaluation and Future Projections. *Clim. Res.* **2015**, *64*, 123–140. [\[CrossRef\]](#)
16. Zittis, G.; Hadjinicolaou, P.; Klangidou, M.; Proestos, Y.; Lelieveld, J. A Multi-Model, Multi-Scenario, and Multi-Domain Analysis of Regional Climate Projections for the Mediterranean. *Reg. Environ. Change* **2019**, *19*, 2621–2635. [\[CrossRef\]](#)
17. Zittis, G.; Bruggeman, A.; Lelieveld, J. Revisiting Future Extreme Precipitation Trends in the Mediterranean. *Weather Clim. Extrem.* **2021**, *34*, 100380. [\[CrossRef\]](#)
18. Zittis, G.; Almazroui, M.; Alpert, P.; Ciais, P.; Cramer, W.; Dahdal, Y.; Fnais, M.; Francis, D.; Hadjinicolaou, P.; Howari, F.; et al. Climate Change and Weather Extremes in the Eastern Mediterranean and Middle East. *Rev. Geophys.* **2022**, *60*, e2021RG000762. [\[CrossRef\]](#)
19. Founda, D.; Varotsos, K.V.; Pierros, F.; Giannakopoulos, C. Observed and Projected Shifts in Hot Extremes’ Season in the Eastern Mediterranean. *Glob. Planet. Change* **2019**, *175*, 190–200. [\[CrossRef\]](#)
20. Coppola, E.; Nogherotto, R.; Ciarlo, J.M.; Giorgi, F.; van Meijgaard, E.; Kadygrov, N.; Iles, C.; Corre, L.; Sandstad, M.; Somot, S.; et al. Assessment of the European Climate Projections as Simulated by the Large EURO-CORDEX Regional and Global Climate Model Ensemble. *J. Geophys. Res. Atmos.* **2021**, *126*, e2019JD032356. [\[CrossRef\]](#)
21. Cos, J.; Doblas-Reyes, F.; Jury, M.; Marcos, R.; Bretonnière, P.-A.; Samsó, M. The Mediterranean Climate Change Hotspot in the CMIP5 and CMIP6 Projections. *Earth Syst. Dyn.* **2022**, *13*, 321–340. [\[CrossRef\]](#)
22. Georgoulas, A.K.; Akritidis, D.; Kalisoras, A.; Kapsomenakis, J.; Melas, D.; Zerefos, C.S.; Zanis, P. Climate Change Projections for Greece in the 21st Century from High-Resolution EURO-CORDEX RCM Simulations. *Atmos. Res.* **2022**, *271*, 106049. [\[CrossRef\]](#)
23. Xoplaki, E.; González-Rouco, J.F.; Luterbacher, J.; Wanner, H. Wet Season Mediterranean Precipitation Variability: Influence of Large-Scale Dynamics and Trends. *Clim. Dyn.* **2004**, *23*, 63–78. [\[CrossRef\]](#)
24. Feidas, H.; Nouloupoulou, C.; Makrogiannis, T.; Bora-Senta, E. Trend Analysis of Precipitation Time Series in Greece and Their Relationship with Circulation Using Surface and Satellite Data: 1955–2001. *Theor. Appl. Climatol.* **2007**, *87*, 155–177. [\[CrossRef\]](#)
25. Kostopoulou, E.; Jones, P.D. Assessment of Climate Extremes in the Eastern Mediterranean. *Meteorol. Atmos. Phys.* **2005**, *89*, 69–85. [\[CrossRef\]](#)
26. Deitch, M.J.; Sapundjieff, M.J.; Feirer, S.T. Characterizing Precipitation Variability and Trends in the World’s Mediterranean–Climate Areas. *Water* **2017**, *9*, 259. [\[CrossRef\]](#)
27. Zittis, G. Observed Rainfall Trends and Precipitation Uncertainty in the Vicinity of the Mediterranean, Middle East and North Africa. *Theor. Appl. Climatol.* **2018**, *134*, 1207–1230. [\[CrossRef\]](#)
28. Mavromatis, T.; Georgoulas, A.K.; Akritidis, D.; Melas, D.; Zanis, P. Spatiotemporal Evolution of Seasonal Crop-Specific Climatic Indices under Climate Change in Greece Based on EURO-CORDEX RCM Simulations. *Sustainability* **2022**, *14*, 17048. [\[CrossRef\]](#)
29. Spinoni, J.; Vogt, J.V.; Naumann, G.; Barbosa, P.; Dosio, A. Will Drought Events Become More Frequent and Severe in Europe? *Int. J. Climatol.* **2018**, *38*, 1718–1736. [\[CrossRef\]](#)
30. Spinoni, J.; Barbosa, P.; Buchignani, E.; Cassano, J.; Cavazos, T.; Christensen, J.H.; Christensen, O.B.; Coppola, E.; Evans, J.; Geyer, B.; et al. Future Global Meteorological Drought Hot Spots: A Study Based on CORDEX Data. *J. Clim.* **2020**, *33*, 3635–3661. [\[CrossRef\]](#)
31. Cook, B.I.; Mankin, J.S.; Marvel, K.; Williams, A.P.; Smerdon, J.E.; Anchukaitis, K.J. Twenty-First Century Drought Projections in the CMIP6 Forcing Scenarios. *Earth’s Future* **2020**, *8*, e2019EF001461. [\[CrossRef\]](#)
32. Lagouvardos, K.; Karagiannidis, A.; Dafis, S.; Kalimeris, A.; Kotroni, V. Ianos—A Hurricane in the Mediterranean. *Bull. Am. Meteorol. Soc.* **2022**, *103*, E1621–E1636. [\[CrossRef\]](#)
33. Jacob, D.; Petersen, J.; Eggert, B.; Alias, A.; Christensen, O.B.; Bouwer, L.M.; Braun, A.; Colette, A.; Déqué, M.; Georgievski, G.; et al. EURO-CORDEX: New High-Resolution Climate Change Projections for European Impact Research. *Reg. Environ. Chang.* **2014**, *14*, 563–578. [\[CrossRef\]](#)

34. Jacob, D.; Teichmann, C.; Sobolowski, S.; Katragkou, E.; Anders, I.; Belda, M.; Benestad, R.; Boberg, F.; Buonomo, E.; Cardoso, R.M.; et al. Regional Climate Downscaling over Europe: Perspectives from the EURO-CORDEX Community. *Reg. Environ. Chang.* **2020**, *20*, 51. [[CrossRef](#)]
35. Vautard, R.; Kadyrov, N.; Iles, C.; Boberg, F.; Buonomo, E.; Bülow, K.; Coppola, E.; Corre, L.; van Meijgaard, E.; Nogherotto, R.; et al. Evaluation of the Large EURO-CORDEX Regional Climate Model Ensemble. *J. Geophys. Res. Atmos.* **2021**, *126*, e2019JD032344. [[CrossRef](#)]
36. Meinshausen, M.; Smith, S.J.; Calvin, K.; Daniel, J.S.; Kainuma, M.L.T.; Lamarque, J.-F.; Matsumoto, K.; Montzka, S.A.; Raper, S.C.B.; Riahi, K.; et al. The RCP Greenhouse Gas Concentrations and Their Extensions from 1765 to 2300. *Clim. Change* **2011**, *109*, 213. [[CrossRef](#)]
37. Rovithakis, A.; Grillakis, M.G.; Seiradakis, K.D.; Giannakopoulos, C.; Karali, A.; Field, R.; Lazaridis, M.; Voulgarakis, A. Future Climate Change Impact on Wildfire Danger over the Mediterranean: The Case of Greece. *Environ. Res. Lett.* **2022**, *17*, 045022. [[CrossRef](#)]
38. Haylock, M.R.; Hofstra, N.; Klein Tank, A.M.G.; Klok, E.J.; Jones, P.D.; New, M. A European Daily High-Resolution Gridded Data Set of Surface Temperature and Precipitation for 1950–2006. *J. Geophys. Res. Atmos.* **2008**, *113*, D20119. [[CrossRef](#)]
39. Cornes, R.C.; van der Schrier, G.; van den Besselaar, E.J.M.; Jones, P.D. An Ensemble Version of the E-OBS Temperature and Precipitation Data Sets. *J. Geophys. Res. Atmos.* **2018**, *123*, 9391–9409. [[CrossRef](#)]
40. Kotlarski, S.; Keuler, K.; Christensen, O.B.; Colette, A.; Déqué, M.; Gobiet, A.; Goergen, K.; Jacob, D.; Lüthi, D.; van Meijgaard, E.; et al. Regional Climate Modeling on European Scales: A Joint Standard Evaluation of the EURO-CORDEX RCM Ensemble. *Geosci. Model Dev.* **2014**, *7*, 1297–1333. [[CrossRef](#)]
41. Katragkou, E.; García-Díez, M.; Vautard, R.; Sobolowski, S.; Zanis, P.; Alexandri, G.; Cardoso, R.M.; Colette, A.; Fernandez, J.; Gobiet, A.; et al. Regional Climate Hindcast Simulations within EURO-CORDEX: Evaluation of a WRF Multi-Physics Ensemble. *Geosci. Model Dev.* **2015**, *8*, 603–618. [[CrossRef](#)]
42. Mann, H.B.; Whitney, D.R. On a Test of Whether One of Two Random Variables Is Stochastically Larger than the Other. *Ann. Math. Statist.* **1947**, *18*, 50–60. [[CrossRef](#)]

Disclaimer/Publisher’s Note: The statements, opinions and data contained in all publications are solely those of the individual author(s) and contributor(s) and not of MDPI and/or the editor(s). MDPI and/or the editor(s) disclaim responsibility for any injury to people or property resulting from any ideas, methods, instructions or products referred to in the content.